

# AN INDEX-BASED SHADOW EXTRACTION APPROACH ON HIGH-RESOLUTION IMAGES

Guangyao DUAN<sup>a, b, c, \*</sup>, Huili GONG<sup>a, b, c</sup>, Wenji ZHAO<sup>a, b, c</sup>, Xinming TANG<sup>d</sup>, Beibei CHEN<sup>a, b, c</sup>

<sup>a</sup> Key Laboratory of 3D Information Acquisition and Application, Ministry of Education, Beijing 100048, China – (duanguangyao06@163.com, gonghl@263.net, zhwenji1215@163.com)

<sup>b</sup> Key Laboratory of Resource Environment and GIS in Beijing Municipal, Beijing 100048, China

<sup>c</sup> College of Resources Environment and Tourism, Capital Normal University, Beijing 100048, China

<sup>d</sup> Satellite Surveying and Mapping Application Center, NASG, Beijing 101300, China

**ABSTRACT:** Focusing on high-resolution satellite images, the paper proposed a method for shadow detection that based on the object-oriented method and the characteristic components. The components such as the color invariant C3, the brightness I, the first principal component PC1 and RATIO<sub>b\_nir</sub> were computed by analyzing the spectral feature of shadows to highlight the shadow areas in the images. For the difference of the construction methods, the value range in each component varies a lot that made it difficult for the comprehensive analysis. To overcome the above weakness, a linear normalization method was employed to transform pixel values of all images into the same range 0-1. On the basis of the above shadows in the highlight image, the Object-Oriented method which was composed of segmentation and information extraction was used for the detection of shadow areas. According to the characteristics of high-resolution images, the brightness I and PC1 component were chosen as the main data source for multi-resolution segmentation. Features such as Mean Value, Maximum Difference, Standard Deviation, Area and Gray Level Co-occurrence Matrix that largely indicated the difference between the shadow and non-shadow objects were selected to separate shadow areas from images. Shadows in twenty Quickbird images of 1000\*1000 pixels were extracted by the proposed method and traditional method. The average total accuracy of such new method was 97%; the average producer accuracy was 96%, and the average Kappa index was 0.94. The result showed that the special-bands-based object-oriented method could obtain shadows with perfect shape that without fragmentation when comparing with the pixel-based method. It had a higher accuracy than the object-oriented method that based on the original optical images.

**KEY WORDS:** Shadow Detection, Spectral Feature, Object-Oriented, Characteristic Components, Color Invariant Indices

## 1. INTRODUCTION

Shadows on high-resolution affects the visual interpretation and automatic identification of ground features. However, it reflects the shape, height, surface character and relative position of interest target in the image. The accuracy identification of shadows is the precondition of their removal and utilization, which means that the research on shadow extraction is very essential.

There are two types of shadow detection algorithms for high-resolution images. The first is based on the spectral characteristics of the image. Researches show that the shadows of different buildings on the images have some common characteristics such as color, shape and brightness, which can be analyzed to extract shadow areas, see e.g., V Tsai.( 2006), P Sarabandi et al. (2004), V Arévalo et al.( 2008). The second comes from the mechanism model of the shadow formation process. The shadow areas can be calculated and distinguished according to some prior knowledge such as the solar elevation, solar azimuth, target features and the sensor parameters, see e.g., V Arévalo et al.( 2008), T Nakajima et al. (2002). In spite of the strong theoretic value of the second method, its application has some limitations for the difficulty in acquiring the solar and target information. In general, the first method is widely used for its simple and direct character.

Inland and foreign researchers do many researches in the extraction of shadows. Take one of the several original bands as input, F Cheng, etc. (1995), V Shettigara, etc. (1998), D Lu (2006) segmented shadows with thresholding method. Although this approach was relatively simple, fixed value was not easily determined for the complex spectral character high resolution imagery exhibits, which would result in some misclassifications. Besides, color space transformation methods have proven very effective in extracting shadows by enhancing the interested information.  $C_1C_2C_3$  color space has been utilized for shadow

detection by combining with region growing method (V Arévalo, etc. 2008) and edge detection method (F Yamazaki, etc. 2004). Wang S G et al. (2003), V Tsai (2006), J Liu et al. (2011) have analyzed the properties of shadow and applied the ISH color space for shadow extraction. Then the KL transformation and principal component analysis(PCA) were also used for enhancing and segmenting shadows by Wang S G et al (2004, 2010). Based on ISH transformation and PCA, Liu H et al. (2013) presented a shadow index with which to segment shadows by means of the thresholding method. Overall, the above methods extracted shadow with one single component which was transformed aiming to highlight the useful information. In spite of the good results some researchers got, the limited features for the distinction of shadows from other objects would result in low extraction accuracy in relative complexity images.

Simultaneously, some multi-feature, multi-band integrated approaches were gradually been used to extract shadows. Guo J H et al. (2006), Wan Y C et al. (2012) proposed multi-band shadow detection method by character bands establishing. Apart from the transformed bands, RGB bands are combined with the intensity and saturation to detect shadows (A Suzuki et al. 2000), the Landsat TM data (TM3, TM4 and TM5) and a panchromatic SPOT were fused to extract shadow information (He G J et al. 2001). There were also some relatively complicated proposed, such as the low-pass filtering techniques in homomorphic system, Spectral Angle Mapper (SAM) algorithm and a combined radial basis function neural networks, see e.g., H Etemadnia et al. ( 2003 ), Huang H et al. (2004 ) and Xia H Y et al. (2011). Although the advantage of avoiding omission and error to some extent by using such methods, there were limitations in the application of shadow detection for their complexity. Most of the above pixel-based methods were carried out by using some image enhancement method. The

\* Corresponding author. Email: duanguangyao06@163.com.

accuracy was limited for the fragmentation of patches, and would be further affected by the post-processing of image classification.

Due to the development of high-resolution remote sensing and the information extraction technology, Pu Z et al. (2008), F Yamazaki et al. (2010, 2012) carried out some experiment of object-oriented shadow extraction. However, they mainly focused on the retrieval of shadow area, and only the original spectral information such as the mean value of each band was used. The results may be of low accuracy when the images were relatively complex.

By analyzing the spectral characteristics of shadows on high-resolution satellite imagery, this paper proposes high-precision

shadow extraction strategies under a certain multi-feature constraint condition according to the characteristic components' establishment and the object-oriented method.

## 2. METHOD

Twenty QuickBird images obtained at three different times are selected by the paper. All the high-resolution satellite images contain four bands(R, G, B and NIR). Test areas of 1000\*1000 pixels that cover ground features of various kinds and complexities are extracted for statistically analyzing the image characters. The average correlation coefficient and standard deviation of twenty images (Table 1) were calculated to avoid the occurrence of accidental error.

CORR	B1		B2		B3		B4	
	CORR	STD	CORR	STD	CORR	STD	CORR	STD
B1	1.000	0.000	0.958	0.025	0.871	0.065	0.594	0.117
B2	0.958	0.025	1.000	0.000	0.950	0.021	0.668	0.112
B3	0.871	0.065	0.950	0.021	1.000	0.000	0.667	0.134
B4	0.594	0.117	0.668	0.112	0.667	0.134	1.000	0.000

Table 1 The average correlation coefficient(CORR) and standard deviation(STD) of twenty images

As seen from the table, there is greater relevance among the first three bands. The correlation coefficients of every two bands are more than 0.85 and the standard deviations are less than 0.1, which reflects the similarity result of the twenty images. The fourth band has weaker correlation and greater standard deviations with the first three bands, meant the difference of the test images. The larger correlation and redundancy between every two bands can lead to lower utilization rate and efficiency of data when processing the raw spectral bands. Therefore, it is necessary to highlight the useful information and reduce the redundancy by means of enhancement, conversion and other processing based on the original data. The paper comprehensively analyzes the characteristics of high resolution remote sensing image and the previous work did by other researchers, and achieves the high-precision extraction of shadows based on the characteristic components' establishment and the object-oriented classification technique. The process is shown in Figure 1.

As can be seen in Figure 1, the main work of the paper is to choose and build indices that reflect shadow characters better and to extract shadows by means of object-oriented technique. The color invariant  $C_3$ , the principal component  $PC_1$ , the intensity  $I$  and the ratio between B band and NIR band  $RATIO_{b_{nir}}$  are selected as the indices. The combination of both made it possible to achieve optimal accuracy of shadow information extraction.

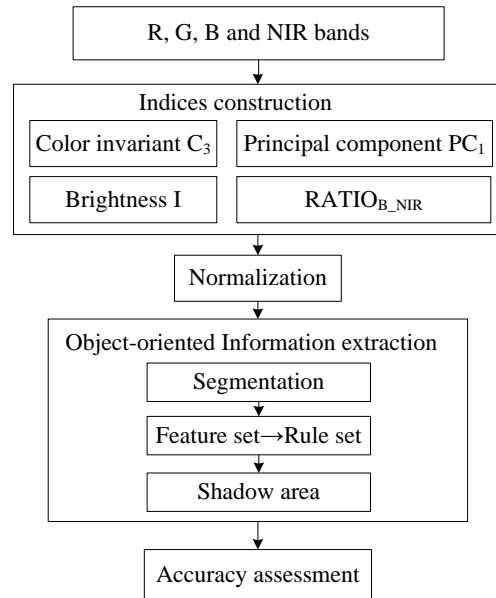


Figure 1. Process of shadow extraction

### 2.1 Analysis and establishment of shadow characteristic components

Shadows in remote sensing images are darker than other targets in vision made it possible to analyze shadow areas using the brightness of ground objects. Because of the dissimilarity of shadow performance at different wavelengths (Figure 2), the spectral analysis method can be used to differentiate shadows from other features. For high-resolution satellite images, certain means of remote sensing enhancement methods based on spectral signatures are beneficial to separate and take full advantage of shadow information.

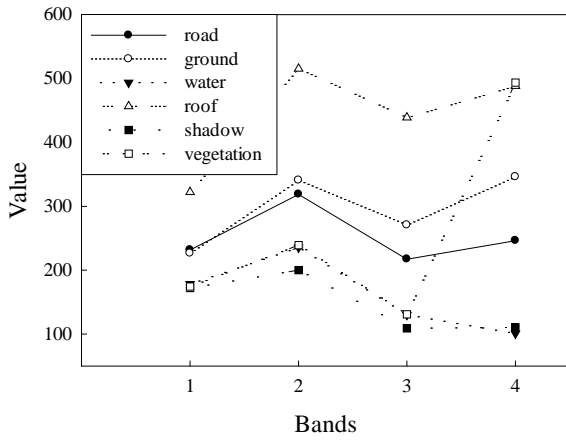


Figure 2 Spectral curves of six ground features

Figure 2 shows that the spectral curves of shadow and water are similar and significantly different from the other surface features. The DN values of shadow and non-shadow areas have the smallest difference in the blue band (band 1) and the biggest difference in the near-infrared band (band 4). There is similar brightness between shadow and vegetation in blue, green and red bands, but significant difference in the near-infrared band. The DN value of water is close to shadow, but a little higher in the first three bands and a little lower in the last band than shadows. Roads, buildings and bare land have greater luminance values than shadows in all bands, which make them easier for distinguishing.

Based on the analysis above, this paper intends to build four special indices, which would highlight shadow information and weaken other factors to improve the success rate of shadow collection.

**2.1.1 The brightness component I:** Since the illumination of shadow area is insufficient, make the value of the shaded area smaller overall than the non-shaded areas. The main contribution of radiation received by the remote sensor is scattered light, not reflected light. The intensity of scattered light is much weaker than reflected light, which makes the shaded area lack of colour information. The brightness component I from ISH space is a good indication of the above character of shadows. The component I can be calculated by equation (1):

$$I = (R + G + B) / 3 \quad (1)$$

Some scholars take advantage of this feature of the shadow to extract the shadow areas by using the threshold segmentation method. However, the phenomenon that different objects in images have the same spectra characteristics makes the extraction result not very satisfactory. The normalized histogram of I component (Figure 3) shows that the DN values of dark areas are relatively concentrated, but with no significant difference from the lighter areas. There are some downsides to extract shadow relying solely on a certain threshold of the brightness component. With the increasing complexity of surface features, threshold between shadows and other surface features is not easy to determine, resulting in larger error results. Therefore, the brightness character is gathered only as one of the components to highlight shadows.

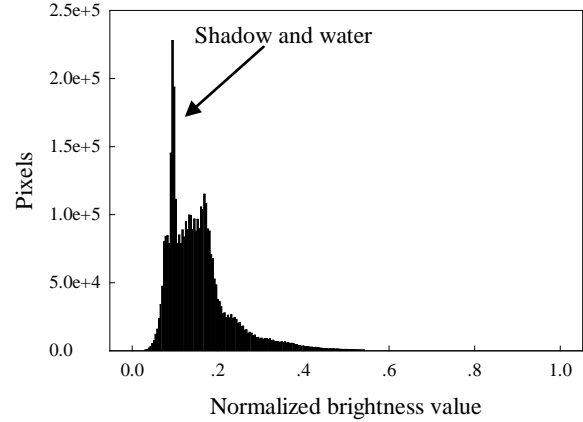


Figure 3 Histogram of brightness value

**2.1.2 The color invariant component  $C_3$ :** When sunlight hits the ground, a series of refraction, reflection and other effects would happen. Remote sensing images are the result of the radiation after complex physical interaction between the incident ray and the surface that received by the sensor. Dichromatic reflection model is a classical model of the process described above. According to this theory, the color invariants can be obtained by constructing a color ratio model to remove the effects of perspective, surface normal, light direction, illumination, reflected light intensity and other factors, etc.

Some color invariant such as HIS,  $C_1C_2C_3$ , rgb,  $l_1l_2l_3$ ,  $m_1m_2m_3$  have been proposed by scholars, at home or abroad, see e.g., T Gevers et al.(1999). Theoretically, these color models are all invariants to a change in viewing direction, object geometry and illumination. The reflection of different wavelengths in the shaded area varies a lot from the non-shaded area, which made it possible to segment shadow regions based on the spectral characteristics of images. V. Arévalo et al. (2008) has confirmed that  $C_3$  component was suitable for shadow extraction. However, the  $C_3$ -band is quite noisy, so it needs some additional auxiliary bands or transformations should be conducted. What is more, the recognition accuracy of shadows by such method mainly depends on the quality of the seed selected, and some good results can be obtained only in the case of the better image quality.

According to the analysis of Dichromatic reflection model and scattering properties of light and the comparison of several color invariant features, the paper considered that the established arctangent index  $C_3$  which take the B-band as numerator and the larger band of R and G as denominator can better reflect the characteristics of the shaded area. However, in spite of the advantage of  $C_3$ , such a single band is not universally appropriate for the extraction of shadows. By the fore analyses, the component is regarded as one of the characters that can aid the extraction of shadows. The  $C_3$  band can be calculated by the following formula (2):

$$C_3 = \arctan \left( \frac{B}{\text{MAX}(R, G)} \right) \quad (2)$$

It can be seen from the luminance histogram (Figure 4) that the  $C_3$  component has the characteristics of concentrated distribution of brightness, approximated brightness of various surface features and unobvious peaks of the histogram. However, the insensitivity to the direct illumination and the ability to distinguish shadow and water to some extent, make such a component important for accurate extraction of shadows.

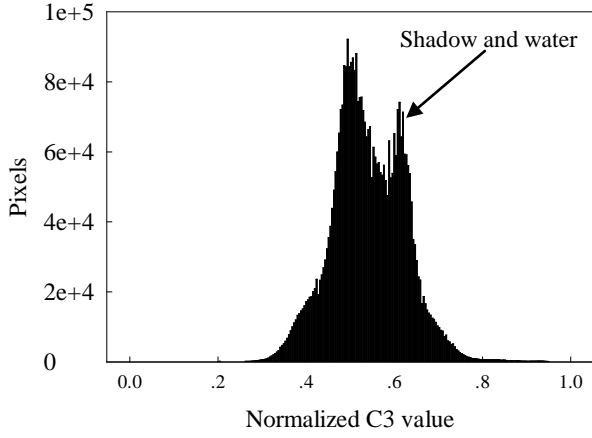


Figure 4 luminance histogram of  $C_3$

**2.1.3 The first Principal component  $PC_1$ :** In view of the high correlation between every two bands of the original image and the inefficiency of such image processing, the principal component analysis method was introduced to reduce the data redundancy, enhance the image contrast and improve the segmentation and extraction accuracy of shadows.

Principal component analysis is such a linear transformation that deals with multi-dimensional data based on the statistical information of images. It can concentrate the information on the bands as few as possible to realize the goal of dimension reduction, on the promise of maintaining most of the original data information. For original Quickbird images, the covariance-based PC method that sent more than 80% information to the first component( $PC_1$ ) was carried out. Therefore, the component  $PC_1$  was selected as one of the characters participated in the extraction of shadows.

Figure 5 shows the spectral curves of several transformed components. The first and second component that contained most of the original information embodied the major differences between various objects. There is little difference of the last two components among the several ground features. What is more, a considerable part of the noise it contains makes it inappropriate for image analysis.

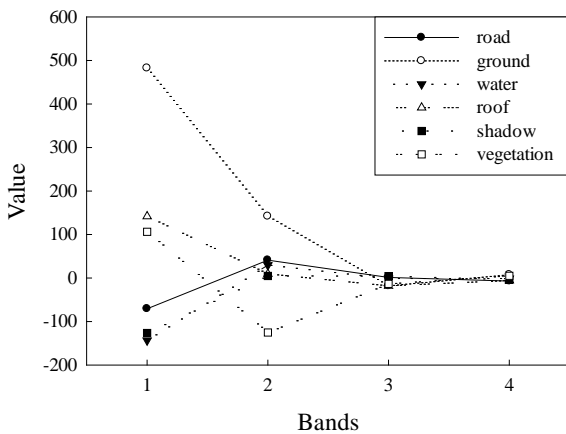


Figure 5 spectral curves of four transformed components corresponding to several ground features

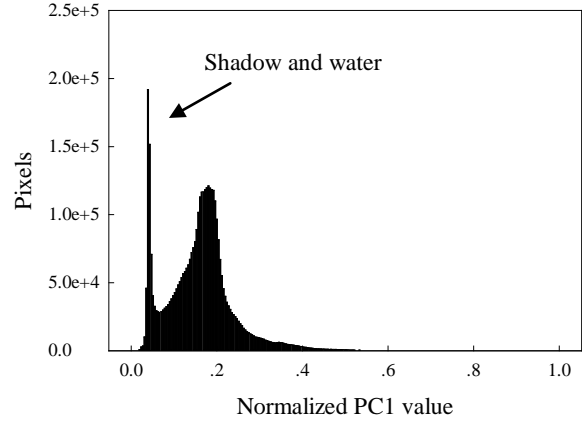


Figure 6 luminance histogram of  $PC_1$

As can be seen from the luminance histogram of  $PC_1$ (Figure 6), the normalized values of shadow and water fluctuate at a quite small range from 0.04 to 0.06. In other words, most of the shadow information is concentrated within this range. As a result, the simple threshold segmentation method can be used to get the initial scope of shadows.

**2.1.4 The  $RATIO_{b\_nir}$  index:** The luminance of each band of the image in shadow areas is lower than non-shadow areas. However, the degree of the brightness reduction varies a lot according to different wavelengths. Such phenomenon is mostly owing to the scattering ability of particles in the air to different wavelengths of light, called the Rayleigh scattering. The Rayleigh scattering mainly studies the scattering effect of particles, which have smaller radii than the wavelength as the incident light. The scattered light intensity and the wavelength have a relationship of inversely proportional to the fourth power, which can be represented as the following formula (3),

$$I(\lambda)_{scattering} \propto \frac{I(\lambda)_{incident}}{\lambda^4} \quad (3)$$

Where  $I(\lambda)_{incident}$  is the intensity distribution function of incident light,

$I(\lambda)_{scattering}$  is the intensity of scattered light,  
 $\lambda$  is the wavelength.

According to the above formula, shorter wavelengths are more likely to be scattered, which means the blue band, one of the several bands in high-resolution images, is strongest scattered by the environment. The light intensity decreases of NIR, R, G bands from the non-shaded area to the shaded area are much more significant than the B-band. Consequently, the subtraction and ratio operation between the several bands can highlight the differences of shaded areas and non-shaded areas. NIR-band, which has the longest wavelength in QuickBird images, has the least scattered light and the lowest DN value in shadow areas, but has similar radiation status with other bands. That is to say, the disparity of the radiation energy of the near-infrared band between the non-hatched region and the shadows are the greatest. As it comes to B-band, as the shortest band, it has the smallest energy difference between shaded area and non-shaded for the reason of Rayleigh scattering. Therefore, the B-band and NIR-band are gathered to build the normalized ratio character ( $RATIO_{b\_nir}$ ), to enhanced shadow details. It is written as below,

$$RATIO_{b\_nir} = \frac{(B - NIR)}{(B + NIR)} \quad (4)$$

Figure 7 shows the histogram of  $RATIO_{b\_nir}$  component containing three obvious peaks. The peak with bigger DN value,

which is distinct separated from the other two, represents the shaded areas.

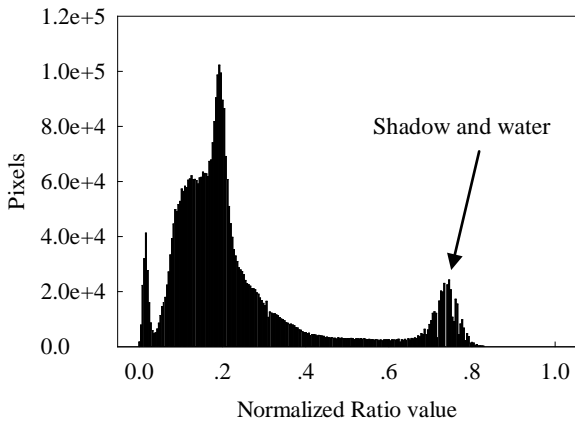


Figure 7 luminance histogram of  $RATIO_{b\_nir}$

**2.1.5 Normalization of each component:** The DN value of each component varies a lot due to the difference of constructed methods, so the analysis of the several combined indices is difficult and not comparable. A transformed method which can unify all values of each component to a certain range is needed to better analyze the data.

A linear normalization method is employed to convert all DN value at a range of 0~1, which can be written as,

$$y = \frac{(x - MinValue)}{(MaxValue - MinValue)} \quad (5)$$

Where  $x$  is the value of each pixel without conversion in every component,

$y$  is the converted value of each pixel in every component,

MinValue is the minimum value of each component,

MaxValue is the maximum value of each component.

## 2.2 Object-oriented shadow extraction:

Object-oriented classification method takes the homogeneous object as the study unit, and aims to extract useful information by developing definite rules. Homogeneous objects, obtained by a certain segmentation algorithm based on the statistical analysis of adjacent pixels, can discriminate the different features on the remote sensing images furthest. The reasonable computing and converting method and the suitable segmentation algorithm set a fundamental for the optimal information extraction. The establishment of corresponding rules based on the full understanding of the spectral, texture and geometric characteristics of the target feature are the guarantee of the result reliability.

The shaded area has been fully enhanced after the set-up of several feature components. With that the object-oriented information extraction is carried out, including segmentation and information extraction.

**2.2.1 Multiresolution segmentation:** A multiresolution segmentation method which can minimize the average heterogeneity of image objects was adopted in this paper. Four parameters such as weights, scale, shape factor and compactness should be set according to the image and targets' characters.

The  $C_3$  and  $RATIO_{b\_nir}$  components are the ratio of just two bands. Some pixels of them could be quite noise in case of the denominator is small that result in the fuzzy of edge to some extent. The two indices are unsuitable for segmentation but information extraction. Therefore, the weights of the  $PC_1$  and brightness components were set as 1 when the  $C_3$  and  $RATIO_{b\_nir}$  components were set as 0.

The scale can be determined according to the types and complexities of surface features on the images. The selection of the optimal scale for segmentation depends on several experiments with the criterion of segmenting different features as far as possible and the requirement that there is not too much fragmentation of one feature. The urban fringe areas, covered by relatively small and complex features, need a smaller-scale parameter. When it comes to the central city areas that covered by comparatively large and regular features, a larger-scale parameter is needed.

The total sum is 1 by adding the shape factor and its opposite, the spectral factor; and the total sum of the two ingredients of shape factor, smoothness and compactness, is also 1. Therefore, the shape and compactness index can fully reflect the consideration of the homogeneity of objects during the segmentation process. The spectral that contains most of the information in remote sensing images is a predominant factor in the segmentation process, and a larger weight should be set. However, the effect of the shape factor in the segmentation process cannot be ignored. It plays an irreplaceable role on maintaining the integrity of the segmentation object, and a parameter of zero values means that only consider the spectral information but regardless of shape information. Compactness index is used to distinguish the compact and non-compact objects, and smoothness index indicates the smoothing treatment of the object edge. A relatively larger value of shape and compactness factor should be set due to the regulation of ground features, and the value of them can be smaller if the ground objects are complex in the images.

**2.2.2 Information Extraction:** Every feature has its characteristic that distinguishes it against other objects. Object-oriented information extraction is the core work after segmentation, mainly by selecting appropriate features to build the rule set and dividing objects with the membership function. Characteristics such as the luminance, standard deviation, maximum difference, area and GLCM of the constructed components are selected to build the rule set.

$PC_1$  and  $I$  components largely reflect the original spectral information of images, and the histograms (Figure 4 and 6) of them show smaller DN-value in shadow and water areas. The values of dark areas in  $PC_1$  component, by contrast, are more centralized and separable. The analysis of the characteristics might make for the crude extract of the shaded area according to the object luminance.

However, for the large fluctuations of DN-values in shadow areas on account of the complexity of features and the similarity of shadows and the water in non-shaded areas, the shadow areas that extracted based on the luminance value of the shaded areas are of great uncertainty and need further correction. As in Figure 5 and 7, shadow and water are brighter in  $C_3$  and  $RATIO_{b\_nir}$  components. Color invariant feature  $C_3$ , which is not sensitive to the complex surface features in shaded areas, can reduce the effect of bright ground features. The shadow areas that generally have smaller areas, smoother texture and greater standard deviation than water make it possible to accurately separate the shaded area by comprehensive analyzing the area, standard deviation and smoothness characters.

The rules for the extraction of shadows are set as bellow in Figure 8 according to the above analysis,

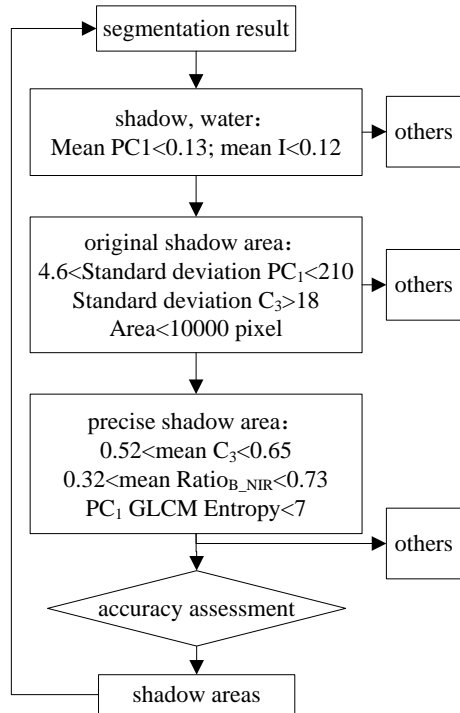


Figure 8 extracting flow of shadows

As can be seen in Figure 8, the object brightness of  $PC_1$ ,  $I$  and  $RATIO_{b\_nir}$  are used to extract the initial shadow areas, the



Figure 9 Shadow areas

#### 4. DISCUSSION

As can be seen in Figure 9, shadows in six images are extracted without fragmentation in visual. There is almost no misclassification in the first two images that contain rather simple ground features. The third and fourth images in Figure 9, which have varying sizes of shadows and relatively complex ground features, also achieve a great classification result. The last two images that obtained in summer contain some relatively lush trees and low buildings. The holes in the shadow areas

standard deviation and area of  $PC_1$  and  $C_3$  are contributed to the removing of some water areas. After that, the GLCM entropy of  $PC_1$  and the mean value of  $C_3$  are used for the refinement of shadow extraction, and the membership function is selected for the fuzzy classification. Finally, the validation and accuracy assessment is carried out to evaluate the shadow extraction result.

### 3. EXPERIMENT AND ANALYSIS

#### 3.1 Experimental Data

Twenty QuickBird images of  $1000 * 1000$  pixels are selected for the shadow extraction experiment in the paper. The data consists of four bands, blue band 450-520nm, green band 520-600nm, red band 630-690nm and near-infrared bands 760-900nm. Twenty images that collected from three different times contained various types of features. High density buildings in downtown area, low-rise houses in urban fringe and vegetation areas are all been taken into consideration by the paper.

#### 3.2 Experimental Results

By combining information extraction of shadow with the object-oriented classification and characteristic component establishment, shadows on twenty images are collected. For the space limitations in the article, six of the twenty results are overlaid on the original RGB image and listed below,

indicate the uncovered canopy which can better reflect the precise accuracy of the extraction results.

The traditional maximum likelihood supervised classification approach was adopted as the comparative experiment, and the accuracy was quantified mainly by the confusion matrix. The average accuracy and its standard deviation of each indicator in the confusion matrix were calculated for the experiment images. The results of maximum likelihood supervised classification

method were listed in Table 2, while the results of the proposed method were listed in Table 3,

Accuracy	Shadow		Nonshadow	
	ACC	STD	ACC	STD
Producer	87.30%	0.128	83.10%	0.124
User	86.06%	0.090	90.01%	0.059
Overall	89.12%	0.033		
Kappa	0.72	0.077		

Table 2 The average accuracy (ACC) and standard deviation (STD) of maximum likelihood supervised classification

The results indicated that the average accuracy of shadows is no more than 90%, and the Kappa coefficient is 0.72. The standard deviations for some indicators have relatively large values, which mean the unstable results. In other words, the supervised classification method can obtain results with accuracies more than 90% for simple images, however, less than 80% for images with complex features and structures.

Accuracy	Shadow		Nonshadow	
	ACC	STD	ACC	STD
Producer	96.08%	0.017	98.36%	0.011
User	96.58%	0.026	97.80%	0.015
Overall	97.53%	0.008		
Kappa	0.94	0.025		

Table 3 The average accuracy (ACC) and standard deviation (STD) of the proposed method

As can be seen from Table 3, the proposed method achieved an accuracy of more than 96% with the Kappa coefficient of 0.94. The standard deviation of classification accuracy was not more than 0.03, indicating stability of the extraction accuracy. That is, images of different acquisition time and different complexity can all get great extraction results with the proposed method. The accurate extraction of shadow information would lay the foundation for the subsequent shadow removal and geometric measurement.

## 5. CONCLUSION:

For the limitations of the previous extraction methods, some special components, which aim to enhance the shadow information as far as possible, were established by means of principal component analysis, color invariant features and space transformation methods according to the spectral characteristics. The brightness character  $I$  and the first principal component  $PC_1$  contained most of the information on the original images. These two elements that built without the ratio measurement of the image bands contained ground features that retained all edge information, and they are more suited as input for segmentation. The shaded area hardly receives direct light but scattered light. At the same time, the color invariant feature  $C_3$ , which was insensitive to direct light, had unique advantages in shadow detection. The  $RATIO_{b_{nir}}$  component that established according to the Rayleigh scattering differences of the blue-band and near-infrared band in shaded areas can significantly enhance the shadow information. The above analysis and establishment of the special components would be very conducive to the final information retrieval.

Characteristics such as the mean value, standard deviation, maximum difference and gray level co-occurrence matrix are selected to build the rule set and carry out the object-oriented extraction of shadows. The rule was set by gathering and

refining multi-features. Proper threshold of each feature that ensures all shadows are contained is set, and the intersection of all features was identified as shadow areas. Such information extraction strategy can make full use of all features, and remove the misclassification as far as possible while obtaining the precise shadow areas.

The paper takes twenty images as experiment data and maximum likelihood method as comparative experiment. Firstly, the results are evaluated visually and quantitatively by the confusion matrix. The result shows that the shadows extracted by traditional method are crushing. The accuracy is not only low but also unstable, and even lower than 80% for complex features in the image. However, the proposed method increases the difference between shadows and other surface features by means of space transformation and image enhancement technology to ensure the accurate extraction of the shadow. Object-oriented method that takes into account the spectral, geometry and texture characteristics of remote sensing images can extract smooth boundary and avoid broken spots, what is more, achieve an average overall accuracy of 97%.

Experimental results showed great superiority of the proposed method for high-resolution images. However, there is still a small amount of misclassifications. For example, the water plants would darken the water, and the emerged plants have shadows themselves. Such objects that have blurred boundaries may be misclassification. Some work may be carried out concentrating on such cases to obtain better results. The removal of shadows and the calculation of building height is the next work.

**Acknowledgements** The research is financially supported by the Natural Science Foundation of China (No.s 41130744, 41171335)

## REFERENCE:

- [1] Zhang X. M., He G. J., Wang W., et al, 2011. Extracting Buildings Height and Distribution Information in Tianjin City from the Shadows in ALOS Images[J]. Spectroscopy and Spectral Analysis. 31(07):2003-2006.
- [2] Tsai V. J. D., 2006. A comparative study on shadow compensation of color aerial images in invariant color models[J]. IEEE Transactions on Geoscience and Remote Sensing. 44(6):1661-1667.
- [3] Sarabandi P., Yamazaki F., Matsuoka M., 2004. Shadow detection and radiometric restoration in satellite high resolution images[J]. 2004 IEEE International Geoscience and Remote Sensing Symposium(IGARSS).
- [4] Arévalo V., González J., Ambrosio G., 2008. Shadow detection in colour high-resolution satellite images[J]. International Journal of Remote Sensing. 29(7):1945-1963.
- [5] Nakajima T., Tao G., Yasuoka Y., 2002. Simulated recovery of information in shadow areas on IKONOS image by combing ALS data[J]. Proceeding of Asian Conference on Remote Sensing (ACRS).
- [6] Cheng F., Thiel K. H., 1995. Delimiting the building heights in a city from the shadow in a panchromatic SPOT image. Part 1: Test of forty two buildings [J]. International Journal of Remote Sensing. 16(3):409-415.
- [7] Lu D., 2006. The potential and challenge of remote sensing-based biomass estimation[J]. International Journal of Remote Sensing. 27(7):1297-1328.
- [8] Shettigara V. K., Sumerling G. M., 1998. Height determination of extended objects using shadows in SPOT

- images[J]. Photogrammetric Engineering and Remote Sensing. 64(1):35-44.
- [9] Gevers T., Smeulders A. W. M., 1999. Robust histogram construction from color invariants[J]. Pattern Recognition. (32):453-464.
- [10] Liu J., Fang T., Li D., 2011. Shadow detection in remotely sensed images based on self-adaptive feature selection[J]. IEEE Transactions on Geoscience and Remote Sensing. 49(12):5092-5103.
- [11] Wang S. G., Guo Z. J., Li D. R., 2003. Extracting Buildings Height and Distribution Information in Tianjin City from the Shadows in ALOS Images[J]. Geomatics and Information Science of Wuhan University. 28(05):514-516.
- [12] Wang S. G., Wang J. L., Guo L. Y., 2004. Shadow Detection of Color Aerial Images Based on K-L Transformation[J]. Journal of Geomatics. 29(02):21-23.
- [13] Wang Y., Wang S. G., 2010. A Shadow Detection Method of Color Image Based on RGB Color Space[J]. Journal of applied sciences. 28(02):136-141.
- [14] Liu H., Xie T. W., 2013. Study on Shadow Detection in High Resolution Remote Sensing Image based on PCA and HIS Model[J]. Remote Sensing Technology and Application. (01):78-84.
- [15] Suzuki A., Shio A., Arai H., Ohtsuka S., 2000. Dynamic shadow compensation of aerial images based on color and spatial analysis[J]. Proceedings of the 15th International Conference on Pattern Recognition Barcelona, Catalonia, Spain. 317-320.
- [16] He G. J., Chen G., He X. Y., et al, 2001. Extracting Buildings Distribution Information of Different Heights in a City from the Shadows in a Panchromatic SPOT Image[J]. Journal of Image and Graphics. 06(05):425-428.
- [17] Guo J. H., Tian Q. J., Wu J. Z., 2006. Study on Multispectral Detecting Shadow Areas and A Theoretical Model of Removing Shadows from Remote Sensing Images[J]. Journal of Remote Sensing. 10(02):151-159.
- [18] Gao X. J., Wan Y. C., Zheng S. Y., 2012. Automatic Shadow Detection and Compensation of Aerial Remote Sensing Images[J]. Geomatics and Information Science of Wuhan University. 37(11):1299-1302.
- [19] Etemadnia H., Alsharif M. R., 2003. Automatic image shadow identification using LPF in homomorphic processing system[J]. 7th Digital Image Computing: Techniques and Applications, Sun C, Talbot H, Ourselin S and Adriaansen T (Eds).
- [20] Huang H., Zhang Y. J., Ma X. M., 2004. A Shadow Automated Extraction Method of IKONOS Images Based on Image Fusion[J]. Remote Sensing Information. (04):29-31.
- [21] Xia H. Y., Guo P., 2011. A shadow detection of remote sensing images based on statistical texture features[J]. Journal of Remote Sensing. 15(04):778-791.
- [22] Pu Z., Yang L., Bai J., 2008. Shadow Detection and Removal Based on Object-oriented Method in High Spatial Resolution Remote Sense Image[J]. Remote Sensing Technology and Application. 23(6):735-737.
- [23] Liu W., Yamazaki F., 2012. Object-based shadow extraction and correction of high-resolution optical satellite images[J]. IEEE Journal of Applied Earth Observations and Remote Sensing. 5(4):1296-1302.
- [24] Liu W., Yamazaki F., 2010. Shadow extraction and correction from quickbird images[J]. 2010 IEEE International Geoscience and Remote Sensing Symposium (IGARSS).